Liquid Crystals
Publication details, including instructions for authors and subscription information:
http://www.informaworld.com/smpp/title~content=t713926090

Solution of the mixed Dirichlet-Neumann problem for molecular orientation in liquid crystals

J. C. Dias[a]; C. A. R. Yednak[a]; E. K. Lenzi[a]; L. R. Evangelista[a]
[a] Departamento de Física, Universidade Estadual de Maringá Avenida Colombo, 5790-87020-900 Maringá (PR), Brazil

To cite this Article Dias, J. C. , Yednak, C. A. R. , Lenzi, E. K. and Evangelista, L. R.(2007) 'Solution of the mixed Dirichlet-Neumann problem for molecular orientation in liquid crystals', Liquid Crystals, 34: 9, 1107 — 1114
To link to this Article: DOI: 10.1080/02678290701616272
URL: http://dx.doi.org/10.1080/02678290701616272

Liquid Crystals, Vol. 34, No. 9, September 2007, 1107–1114

Taylor & Francis
Taylor & Francis Group

Solution of the mixed Dirichlet–Neumann problem for molecular orientation in liquid crystals

J.C. DIAS, C.A.R. YEDNAK, E.K. LENZI and L.R. EVANGELISTA

Departamento de Física, Universidade Estadual de Maringá Avenida Colombo, 5790-87020-900 Maringá (PR), Brazil

(*Received 28 May 2007; accepted 7 August 2007*)

The orientation of the nematic director field under the action of an external time-dependent field is theoretically investigated as a mixed Dirichlet–Neumann boundary-value problem. This mathematical problem represents the situation in which a nematic liquid crystal sample is limited by two inhomogeneous flat surfaces, separated by a distance d, on which the anchoring is weak. By considering the one-constant approximation and a parabolic approximation for the surface energy, the initial conditions and boundary-value problem for the profile of the tilt angle can be analytically solved even in the case in which the surfaces are not identical, which represents the more general situation. The results are valid for small deviations from the homeotropic orientation and for $\theta-\Theta \ll 1$, where θ is the actual tilt angle and Θ characterizes the easy direction imposed by the surface, and can be relevant to investigation of the molecular orientation in a nematic cell submitted to a small external voltage.

1. Introduction

Recently, many works have approached boundary-value problems in connection with molecular orientation in typical nematic liquid crystal (NLC) cells. The problems arise in the framework of the elastic continuum theory for liquid crystalline materials and, in their mathematical formulation, the variational principle to minimize the total elastic energy is invoked [1–9]. This total energy depends on the spatial distribution of the director **n**, which represents the average molecular orientation in the cell. The equilibrium configuration for the director distribution can be influenced by the orientation imposed by the surface treatment in typical cells that are usually formed by two flat (treated) surfaces separated by a distance d, in the shape of a slab [10–13].

The mixed Dirichlet–Neumann *problem* in this context refers to the situation in which the anchoring of the director at the surfaces is weak, i.e. the surface energy is a finite quantity. Thus, the total elastic energy to be minimized is composed by a contribution coming from the bulk energy added to the surface energies. In this more difficult mathematical problem, the angles determining the molecular orientation at the surfaces are not fixed by the boundary conditions. Particular cases obtained as limiting situations of this more general problem have been extensively discussed in recent years [14–20]. In this paper, we present the complete analytical solutions for this class of problems in terms of Green's functions, by taking into account the usual contributions that intervene in real physical situations. For this reason, the analysis is carried out by considering that the cell is subjected to a time-dependent external electric field, the viscous torque is taken into account also when the surfaces, which are not identical, are characterized by a space–time-dependent distribution of the easy axes and, as outlined above, the situation is of weak anchoring. On the other hand, the deformations are restricted to remain in a plane, i.e. we consider only splay–bend deformations, in the one-constant approximation; furthermore, the surface energy is the parabolic approximation for the usual Rapini–Papoular expression [21]. In this manner, the results are valid for small deviations from the homeotropic orientation, i.e. for $\theta \ll 1$ and for $\theta-\Theta \ll 1$, where θ is the actual value of tilt angle and $\Theta \ll 1$ characterizes the easy direction imposed by the surface. Furthermore, the analysis could be relevant to a cell in which the applied field is very small when compared with the Fréedericksz threshold field to induce deformations in the nematic structure [22, 23].

This paper is organized as follows. In section 2 the total energy and the fundamental equations are established. In section 3 the general solution of the mixed Dirichlet–Neumann problem is given by means of the Green function method. To use the formalism

Liquid Crystals
ISSN 0267-8292 print/ISSN 1366-5855 online
http://www.tandf.co.uk/journals
DOI: 10.1080/02678290701616272

developed in this section, some illustrative examples are discussed in section 4. Some general conclusions are discussed in section 5.

2. Total energy

The elastic energy density of a NLC cell is given by the Frank elastic energy density [1, 2, 25, 26] which, for splay–bend distortions and neglecting surface-like terms, reduces to

$$f=\frac{1}{2}\left\{K_{11}\left(\vec{\nabla}\cdot\mathbf{n}\right)^2+K_{33}\left[\mathbf{n}\times\left(\vec{\nabla}\times\mathbf{n}\right)\right]^2\right\}, \qquad (1)$$

in which $\mathbf{n}$ is a unit vector representing the average molecular orientation of the nematic phase, called director. Furthermore, K_{11} and K_{33}, are, respectively, the bulk elastic constant of splay and bend.

In this situation, the director is everywhere parallel to the $(x-z)$ plane, i.e. $\mathbf{n}=\mathbf{n}(x, z)$. The Cartesian reference frame is chosen with the z-axis normal to the surfaces, located at $z=\pm d/2$. The x-axis is parallel to the direction along which the surface tilt angle is expected to change and is such that $\mathbf{n}=\sin[\theta(x, z)]\mathbf{i}+\cos[\theta(x, z)]\mathbf{k}$, where $\mathbf{i}$ and $\mathbf{k}$ are the unit vectors parallel to the x- and z-axes, respectively (see figure 1).

When the sample is submitted to an external time-dependent electric field $\mathbf{E}(t)$, parallel to the z-axis, another contribution to the elastic energy density, having the form

$$f_E=-\frac{1}{2}\epsilon_a(\mathbf{n}\cdot\mathbf{E})^2=-\frac{1}{2}\epsilon_a\mathbf{E}(t)^2\cos^2\theta, \qquad (2)$$

has to be added to f to complete the bulk elastic energy density. In (2), $\epsilon_a=\epsilon_{\|}-\epsilon_{\perp}$ ($\|$ and $\perp$ refer to the direction of $\mathbf{n}$) is the dielectric anisotropy. The surface energy is usually assumed in the form proposed by Rapini–Papoular [21], written here in the parabolic approximation as

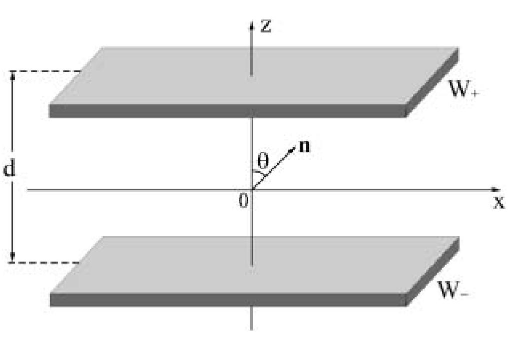

Figure 1. Nematic sample in the shape of a slab of thickness d. The surfaces are characterized by anchoring energies $W_\pm$ and by a space–time-dependent distribution of easy axes: $\Theta_\pm(x, t)$.

$$f_S=\frac{1}{2}W_\pm\sin^2(\theta_\pm-\Theta_\pm)\approx\frac{1}{2}W_\pm(\theta_\pm-\Theta_\pm)^2, \qquad (3)$$

when the actual values of the tilt angle at the surfaces, i.e. $\theta_\pm=\theta(x, z=\pm d/2, t)$ are close to the angles defining the easy directions $\Theta_\pm$ on the surfaces characterized by the anchoring energies $W_\pm$. In the one-constant approximation, $K_{11}=K_{33}=K$, the total energy of the cell, per unit length along y, in the limit of small θ, i.e. for orientations close to homeotropic, is given by

$$\begin{aligned}F=&\int_{-\infty}^{+\infty}\mathrm{d}x\int_{-d/2}^{d/2}\left[\frac{1}{2}K\left(\vec{\nabla}\theta\right)^2+\frac{\epsilon_a}{2}E^2(t)\theta^2\right]\mathrm{d}z\\&+\int_{-\infty}^{+\infty}\frac{1}{2}\left[W_+[\theta(x)-\Theta_+(x)]^2+W_-[\theta(x)-\Theta_-(x)]^2\right]\mathrm{d}x.\end{aligned} \qquad (4)$$

By minimizing (4), taking into account the viscous torque [27], we find the equation for the dynamical evolution of the orientation induced by the electric field

$$\nabla^2\theta(x, z;\ t)-\alpha^2\theta(x, z;\ t)=\frac{\partial\theta(x, z;\ t)}{\partial t}, \qquad (5)$$

written in a non-dimensional form by introducing reduced coordinates $x\to x/d$, $z\to z/d$ and a reduced time $t\to t/\tau_v$, where $\tau_v=\lambda d^2/K$ is the viscous relaxation time and λ is an effective viscosity coefficient of the liquid crystal [27]. In (5) we have introduced the quantity

$$\alpha^2(t)=\pi\left[\frac{E(t)}{E_c}\right]^2, \qquad (6)$$

in which $E_c=\pi/d\sqrt{K/\epsilon_a}$ is the threshold field for the Fréedericksz transition in the strong anchoring case [1]. The solution of (5) is the function $\theta(x, z; t)$ subjected to an initial condition and satisfying appropriated boundary conditions. If these boundary conditions refer to the case of strong anchoring, the mathematical problem is the Dirichlet problem; if, on the other hand, they concern the weak anchoring situation, we have the mixed Dirichlet–Neumann problem hereafter considered.

3. Mixed Dirichlet–Neumann problem

Let us address our investigation to the dynamic reorientation of the nematic director in a cell subjected to an external time-dependent electric field having boundary conditions relevant to the case of weak anchoring. The boundary conditions to be satisfied by the solution of (5) are

$$\pm L_\pm\frac{\partial}{\partial z}\theta(x, z;\ t)+\theta(x, z;\ t)\Big|_{z=\pm 1/2}=\Theta_\pm(x, t), \qquad (7)$$

where $L_\pm=K/(W_\pm d)$ are the extrapolation lengths

($b = K/W$; see [28]) measured in units of the thickness of the sample. To keep the generality, in the present analysis we consider the initial condition $\theta(x, z, 0) = \theta_0(x, z)$. These conditions are very general in the sense that they take two extrapolation lengths into account and require that the distribution of easy axes on the surfaces have a time dependence, in addition to the spatial dependence accounting for inhomogeneities. This time dependence in the easy direction describes the situation in which the easy angle on the surface may change direction continuously under the action of some external agent, for instance, by illuminating a surface covered with some photopolymeric films. Particular cases of (7) have been worked out in [20].

To face this more general problem, we use the Fourier transform and perform the change

$$\theta(k, z;\ t) = e^{-k^2 t - \int_0^t \mathrm{d}\bar{t}\alpha^2(\bar{t})}\overline{\theta}(k, z;\ t), \tag{8}$$

where $\theta(k, z;\ t) = \mathcal{F}\{\theta(x, z;\ t)\}$, with

$$\mathcal{F}\{\cdots\} = \int_{-\infty}^{\infty} \cdots e^{-ikx}\,\mathrm{d}x$$

denoting the Fourier transform. In this manner, by using the Fourier transform and (8) in (5) we obtain

$$\frac{\partial^2}{\partial z^2}\overline{\theta}(k, z;\ t) = \frac{\partial}{\partial t}\overline{\theta}(k, z;\ t), \tag{9}$$

subjected to the boundary condition

$$L_\pm \frac{\partial}{\partial z}\overline{\theta}(k, z;\ t) = \overline{\theta}(k, z;\ t)\Big|_{z=\pm 1/2} = \mathcal{F}_\pm(k, t), \tag{10}$$

with $\mathcal{F}_\pm(k, t) = \Theta_\pm(k, t)e^{k^2 t + \int_0^t \mathrm{d}\bar{t}\alpha^2(\bar{t})}$ and the initial condition $\bar{\theta}(k, z, 0) = \theta_0(k, z)$. Now, we apply the Laplace's transform in (9) to reduce the partial differential equation to an ordinary differential equation and consequently simplify our calculations. By applying the Laplace transform in (9), we obtain the non-homogeneous equation

$$\frac{d^2}{\mathrm{d}z^2}\overline{\theta}(k, z;\ s) - s\overline{\theta}(k, z;\ s) = -\overline{\theta}_0(k, z;\ s). \tag{11}$$

To find the solution for the above equation we use the Green function approach [29, 30] which makes it possible to obtain how the system evolves over time and gives the contribution of the surface to the director field. The Green function $\widetilde{\mathcal{G}}(z, z';\ s)(\widetilde{\mathcal{G}}(z, z';\ s) = \mathcal{L}\{\mathcal{G}(z, z';\ t)\}$ where $\mathcal{L}\{\cdots\} = \int_0^\infty \cdots e^{-st}\,\mathrm{d}t$ is the Laplace transform) used to obtain the solution of (9) is determined from the equation

$$\frac{d^2}{\mathrm{d}z^2}\widetilde{\mathcal{G}}(z, z';\ s) - s\widetilde{\mathcal{G}}(z, z';\ s) = \delta(z - z'), \tag{12}$$

subjected to the boundary condition

$$L_\pm \frac{d}{\mathrm{d}z}\widetilde{\mathcal{G}}(z, z';\ s) + \widetilde{\mathcal{G}}(z, z';\ s)\Big|_{z=\pm 1/2} = 0. \tag{13}$$

After some calculations it is possible to show, by using (13) and (12), that the solution of (9) is formally given by

$$\begin{aligned}\overline{\theta}(k, z;\ s) = &-\int_{-1/2}^{1/2} \mathrm{d}z'\overline{\theta}_0(k, z')\widetilde{\mathcal{G}}(z, z';\ s)\\ &-\frac{1}{L_+}\widetilde{\mathcal{G}}\left(\frac{1}{2}, z;\ s\right)\widetilde{\mathcal{F}}_+(k, s)\\ &-\frac{1}{L_-}\widetilde{\mathcal{G}}\left(-\frac{1}{2}, z;\ s\right)\widetilde{\mathcal{F}}_-(k, s),\end{aligned} \tag{14}$$

where $\widetilde{\mathcal{F}}_\pm(k, s) = \mathcal{L}\{\mathcal{F}_\pm(k, t)\}$; the first term is due to the initial condition and the last two terms are surface contributions. Applying the inverse Laplace transform in (14), we find

$$\begin{aligned}\overline{\theta}(k, z;\ t) = &-\int_{-1/2}^{1/2} \mathrm{d}z'\overline{\theta}_0(k, z')\mathcal{G}(z, z';\ t)\\ &-\frac{1}{L_+}\int_0^t \mathrm{d}\bar{t}\mathcal{G}\left(\frac{1}{2}, z;\ t - \bar{t}\right)\mathcal{F}_+(k, \bar{t})\\ &-\frac{1}{L_-}\int_0^t \mathrm{d}\bar{t}\mathcal{G}\left(-\frac{1}{2}, z;\ t - \bar{t}\right)\mathcal{F}_-(k, \bar{t}).\end{aligned} \tag{15}$$

By substituting (15) into (8) and inverting the Fourier transform, we obtain

$$\begin{aligned}\theta(x, z;\ t) = &-\int_{-1/2}^{1/2} \mathrm{d}z'\theta_0(x, z')\mathcal{G}(z, z';\ t)\\ &-\frac{1}{L_+}\int_0^t \mathrm{d}\bar{t}\int_{-\infty}^{\infty} \mathrm{d}\bar{x}\mathcal{G}\left(\frac{1}{2}, z;\ t - \bar{t}\right)\\ &\times e^{\int_0^{\bar{t}} \mathrm{d}\bar{t}\alpha^2(\bar{t}) - \int_0^t \mathrm{d}\bar{t}\alpha^2(\bar{t})}\widetilde{\mathcal{G}}(x - \bar{x};\ t - \bar{t})\Theta_+(\bar{x}, \bar{t})\\ &-\frac{1}{L_-}\int_0^t \mathrm{d}\bar{t}\int_{-\infty}^{\infty} \mathrm{d}\bar{x}\mathcal{G}\left(-\frac{1}{2}, z;\ t - \bar{t}\right)\\ &\times e^{\int_0^{\bar{t}} \mathrm{d}\bar{t}\alpha^2(\bar{t}) - \int_0^t \mathrm{d}\bar{t}\alpha^2(\bar{t})}\widetilde{\mathcal{G}}(x - \bar{x};\ t - \bar{t})\Theta_-(\bar{x}, \bar{t}).\end{aligned} \tag{16}$$

where $\widetilde{\mathcal{G}}(x, t) = e^{-x^2/(4t)}\Big/\sqrt{4\pi t}$. The Green function for $z' < z \le \frac{1}{2}$ is

$$\mathcal{G}(z, z';\ t) = 2\sum_{n=1}^{\infty} \frac{g_n^{(-)}(z)g_n^{(+)}(z')}{\Delta_n}e^{-k_n^2 t}, \tag{17}$$

and, for $-\frac{1}{2} \leq z < z'$, it is

$$\mathcal{G}(z, z';\ t) = 2\sum_{n=1}^{\infty} \frac{g_n^{(+)}(z) g_n^{(-)}(z')}{\Delta_n} e^{-k_n^2 t}, \tag{18}$$

where

$$g_n^{(\mp)}(z) = \sin\left[k_n\left(\frac{1}{2} \mp z\right)\right] + L_{\pm} k_n \cos\left[k_n\left(\frac{1}{2} \mp z\right)\right] \tag{19}$$

and

$$\begin{aligned} \Delta_n = {} & \left[1 + (L_+ + L_-) - L_+ L_- k_n^2\right]\cos(k_n) \\ & - [(L_+ + L_-) + 2L_+ L_-] k_n \sin(k_n). \end{aligned} \tag{20}$$

The eigenvalues k_n are the roots of the equation

$$\tan k_n = \frac{k_n(L_+ + L_-)}{k_n^2 L_+ L_- - 1}. \tag{21}$$

Note that (16) extends the results reported in [20] and, in the limit $L_+ \to 0$ and $L_- \to 0$, the situation of strong anchoring in both surfaces is recovered, but now incorporating a time dependence on the boundary condition.

4. Illustrative applications

In this section, we apply the formalism developed in the preceding sections to find exact solutions of some representative physical problems in liquid crystals.

4.1. *Uniform orientation in the absence of an external field*

The simplest case refers to $\alpha(t) = 0$ and $\theta(x, z, 0) = 0$. Then, the solution (16), by considering $\Theta_+(\bar{x}) = \Theta_0$ and $\Theta_-(\bar{x}) = \Theta_1$, will be

$$\begin{aligned} \theta(x, z;\ t) = & -\frac{\Theta_0}{L_+}\int_0^t d\bar{t}\,\mathcal{G}\left(\frac{1}{2}, z;\ t - \bar{t}\right) h(x, t - \bar{t}) \\ & - \frac{\Theta_1}{L_-}\int_0^t d\bar{t}\,\mathcal{G}\left(-\frac{1}{2}, z;\ t - \bar{t}\right) h(x, t - \bar{t}), \end{aligned} \tag{22}$$

where

$$h(x, t - \bar{t}) = \frac{1}{\sqrt{4\pi(t - \bar{t})}} \int_{-\infty}^{+\infty} d\bar{x}\, e^{-(x - \bar{x})^2 / 4(t - \bar{t})}. \tag{23}$$

By performing the $\bar{x}$ integration in (22), we obtain

$$\begin{aligned} \theta(x, z;\ t) = & -\frac{\Theta_0}{L_+}\int_0^t d\bar{t}\,\mathcal{G}\left(\frac{1}{2}, z;\ t - \bar{t}\right) \\ & - \frac{\Theta_1}{L_-}\int_0^t d\bar{t}\,\mathcal{G}\left(-\frac{1}{2}, z;\ t - \bar{t}\right). \end{aligned} \tag{24}$$

This solution gives the tilt angle profile, in a NLC sample, for the weak anchoring case in the absence of an external field. This particular situation could be realized experimentally by using an electric field to prepare an initial configuration of the tilt angle, i.e. $\theta(x, z, 0) = \theta_0(x, z)$, and, after that, removing the electric field applied in the system. The relaxation of the liquid crystal present in the sample is governed by (5) with $\alpha(t) = 0$ which, by preparing the experimental sample with suitable choice of Θ_0 and Θ_1 and $\theta(x, z, 0)$, has the solution given by (22). A particular tilt angle distribution is shown in figure 2.

4.2. *Uniform orientation in the presence of an external field*

As a second example, we consider the system submitted to an external, constant and small electric field with $\theta(x, z, 0) = 0$ as in the previous application. Then, the general solution (16) will be

$$\begin{aligned} \theta(x, z;\ t) = & -\frac{\Theta_0}{L_+}\int_0^t d\bar{t}\,\mathcal{G}\left(\frac{1}{2}, z;\ t - \bar{t}\right) e^{-\alpha_0^2 (t - \bar{t})} \\ & - \frac{\Theta_1}{L_-}\int_0^t d\bar{t}\,\mathcal{G}\left(-\frac{1}{2}, z;\ t - \bar{t}\right) e^{-\alpha_0^2 (t - \bar{t})}. \end{aligned} \tag{25}$$

where $\alpha(t)$ is given by (6). Equation (25) represents the tilt angle profile in a nematic sample, in the presence of a small constant external field, with uniform orientation of the easy axes. A typical tilt angle distribution is shown in figure 3 for a particular set of parameters.

4.3. *Periodic distribution in the easy axes*

Let us consider now two illustrative examples dealing with periodic distribution of the easy axes. The first case

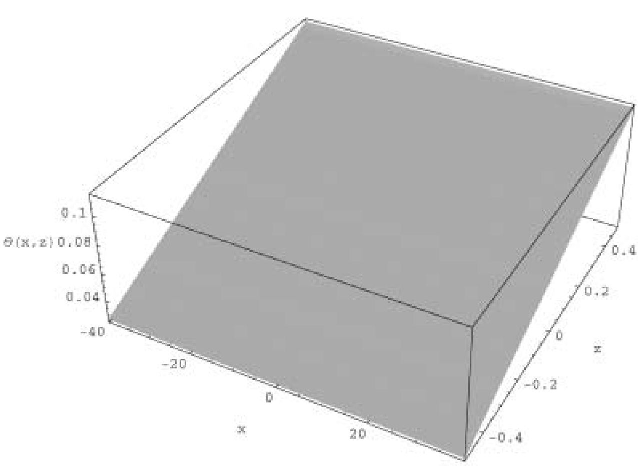

Figure 2. Tilt angle profile $\theta(x, z, t)$ for $\Theta_0 = \pi/10$ in the upper surface and $\Theta_1 = 0$ in the lower surface. The figure was drawn for $t = 5.0$.

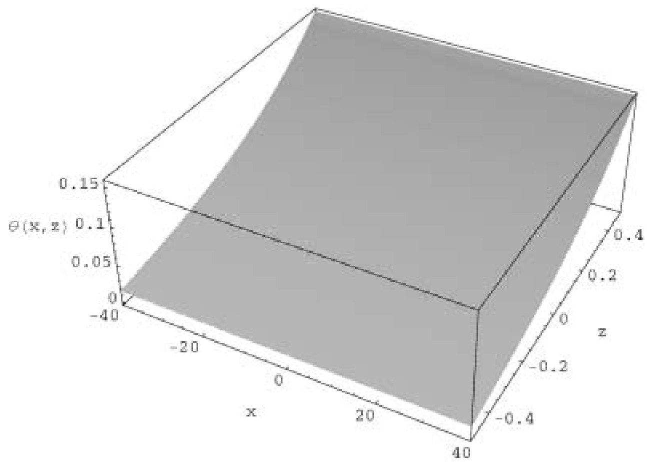

Figure 3. Tilt angle profile $\theta(x, z, t)$ for $\Theta_0=\pi/10$ in the upper surface and $\Theta_1=0$ in the lower surface. The figure was drawn for $\alpha_0=2.0$, $L_+=0.5$, $L_-=0.3$ and $t=2.0$.

refers to a step-like distribution and the second case to a sinusoidal distribution. Both cases are investigated under the action of a constant and small external field. The upper surface is supposed to be treated in order to impose a uniform orientation characterized by Θ_0, whereas the lower surface is characterized by a periodic distribution of easy angle in the form $\Theta_-(\bar{x})$, as represented in figure 4.

We consider first the case in which

$$\Theta_+(\overline{x})=\Theta_0 \quad \text{and} \quad \Theta_-(\overline{x})=\begin{cases}\Theta_1, & 0\leq x\leq a,\\ \Theta_2, & a\leq x\leq 2a,\end{cases} \tag{26}$$

that can be written as

$$\begin{aligned}&\Theta_+(\overline{x})=\Theta_0\\ &\Theta_-(\overline{x})=\Theta_1+(\Theta_2-\Theta_1)\sum_{n=0}^{\infty}(-1)^n F[n,\overline{x}],\end{aligned} \tag{27}$$

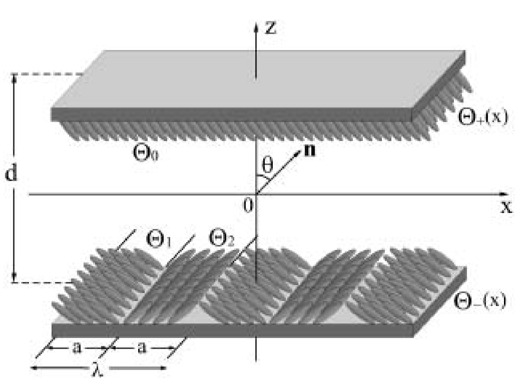

Figure 4. Nematic sample of thickness d whose upper surface is characterized by a uniform distribution of the easy axis whereas the lower surface is characterized by a periodic distribution of easy axis. The spatial periodicity is λ.

where

$$F[n,\overline{x}]=[H(\overline{x}-na)+H(-\overline{x}-(n+1)a)]$$

and $H(\bar{x})$ is the Heaviside's function. By using the boundary conditions (27) in (16) and $\theta(x, z, 0)=0$ one obtains the closed solution

$$\begin{aligned}\theta(x,z;\,t)=&-\frac{\Theta_0}{L_+}\int_0^t \mathrm{d}\bar{t}\,\mathcal{G}\left(\frac{1}{2},z;\,t-\bar{t}\right)e^{-\alpha_0^2(t-\bar{t})}\\ &-\frac{\Theta_1}{L_-}\int_0^t \mathrm{d}\bar{t}\,\mathcal{G}\left(-\frac{1}{2},z;\,t-\bar{t}\right)e^{-\alpha_0^2(t-\bar{t})}\\ &-\frac{\Theta_2-\Theta_1}{2L_-}\sum_{m=0}^{\infty}(-1)^m\\ &\int_0^t \mathrm{d}\bar{t}\,\mathcal{G}\left(-\frac{1}{2},z;\,t-\bar{t}\right)e^{-\alpha_0^2(t-\bar{t})}\\ &\times\left\{\left[1-\mathrm{Erf}\left(\frac{ma-x}{2\sqrt{t-\bar{t}}}\right)\right]\right.\\ &\left.+\left[1-\mathrm{Erf}\left(\frac{x+ma+a}{2\sqrt{t-\bar{t}}}\right)\right]\right\},\end{aligned} \tag{28}$$

representing the profile of the tilt angle. In figure 5, the behaviour of $\theta(x, z, t)$ is shown for illustrative purpose.

Finally, let us consider the periodic distribution of easy axes in the form

$$\Theta_+(\overline{x})=\Theta_0 \quad \text{and} \quad \Theta_-(\overline{x})=\Theta_1\sin[q\overline{x}], \tag{29}$$

where $q=2\pi/\lambda$, with λ being the periodicity of the distribution. By using the boundary conditions (29) in (16) and $\theta(x, z, 0)=0$ one obtains

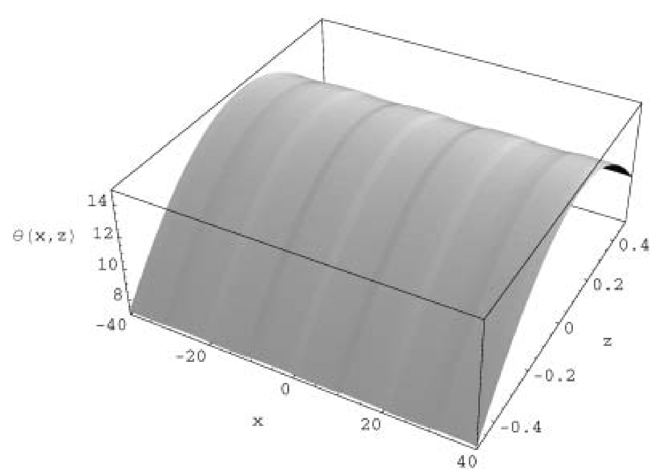

Figure 5. Tilt angle distribution $\theta(x, z, t)$ given by (28), drawn for $\Theta_0=\pi/10$, $\Theta_1=\pi/15$, $\Theta_2=-\pi/15$, $\alpha_0=1.0$, $L_+=0.5$, $L_-=0.3$ and $t=2.0$.

$$\theta(x,z;\ t) = -\frac{\Theta_0}{L_+}\int_0^t \mathrm{d}\bar{t}\mathcal{G}\left(\frac{1}{2}, z;\ t-\bar{t}\right)e^{-\alpha_0^2(t-\bar{t})} + \frac{\Theta_1}{L_-}\int_0^t \mathrm{d}\bar{t}\mathcal{G}\left(-\frac{1}{2}, z;\ t-\bar{t}\right)e^{-\left(\alpha_0^2+q^2\right)(t-\bar{t})}\sin[qx]. \quad (30)$$

In figures 6 (a) and 7 (a), $\theta(x, z, t)$ is shown for some particular values of the parameters. In figure 6 (a), the periodicity is large and the entire sample tends to be distorted, but a more uniform orientation can be found at the upper surface. In figure 7 (a), the periodicity of the distribution of the easy axes is small, the distortion is strongly localized at the lower surface and decreases as one moves away from it. The general solution (30) in the limit $L_+ \to \infty$ reduces to

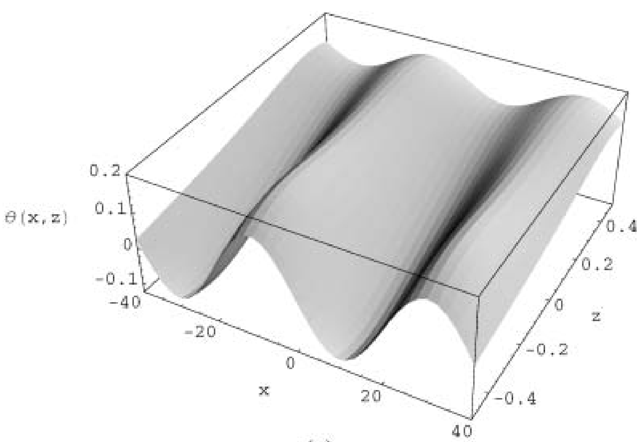

(*a*)

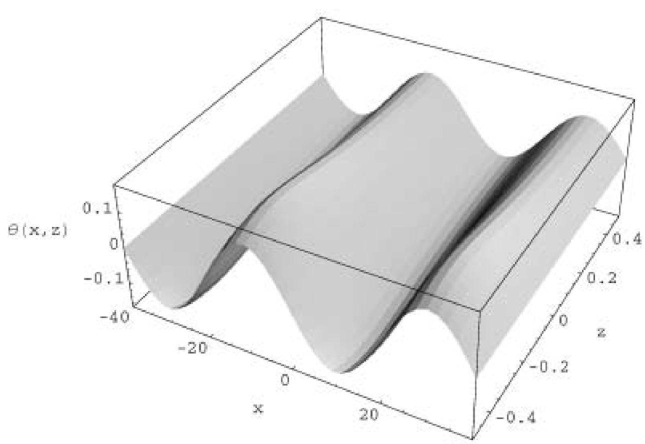

(*b*)

Figure 6. (a) Tilt angle profile $\theta(x, z)$ for $t=5$, with $q=2\pi/\lambda=0.05\pi$, $\Theta_0=\Theta_1=\pi/10$, $L_+=0.5$, $L_-=0.3$ and $a=20.0L_+$. (b) The same as (a), but for the case of no anchoring at the upper surface, i.e. $L_+ \to \infty$.

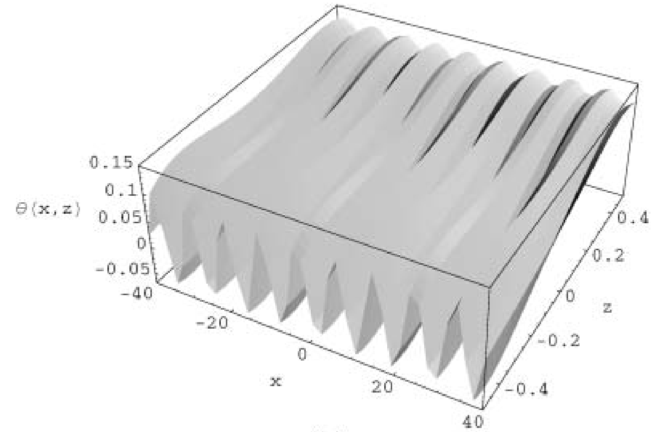

(*a*)

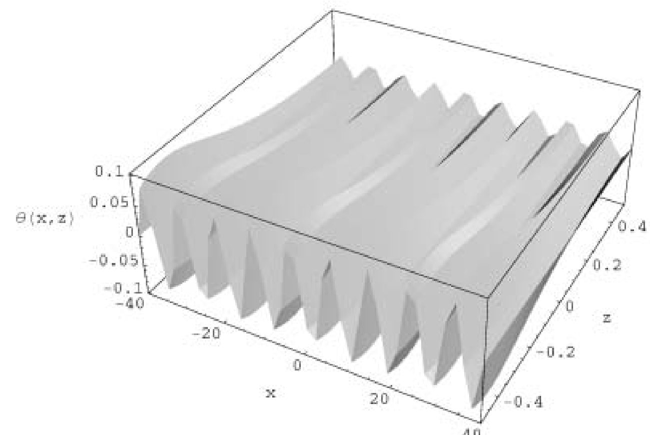

(*b*)

Figure 7. (a) Tilt angle profile $\theta(x, z)$ for $t=5$, with $q=2\pi/\lambda=0.75\pi$, $\Theta_0=\Theta_1=\pi/10$, $L_+=0.5$, $L_-=0.3$ and $a=20.0L_+$. (b) The same as (a), but for the case of no anchoring at the upper surface, i.e. $L_+ \to \infty$.

$$\theta(x,z;\ t) = \frac{2\Theta_1}{L_-}\sum_{n=1}^{\infty} f_-(k_n, z)\left(\frac{1-e^{-\left(k_n^2+\alpha_0^2+q^2\right)t}}{k_n^2+\alpha_0^2+q^2}\right)\sin[qx], \quad (31)$$

where

$$f_-(k_n, z) = \frac{g_n^{(+)}(z)}{\Upsilon_n}k_n\cos[k_n] \quad (32)$$

with $g_n^{(+)}(z)$ given by (19), and

$$\Upsilon_n = \left[1 - L_- k_n^2\right]\cos(k_n) - [1 + 2L_-]k_n\sin(k_n). \quad (33)$$

The case considered in figure 6 (b) refers to a situation in which there is no anchoring at the upper surface. As the periodicity is large, the sample is completely distorted: the entire sample orientation follows the orientation imposed by the lower surface, whose extrapolation length is about one-third of the thickness of the sample. Finally, a similar situation is depicted in figure 7 (b), but the periodicity is smaller than that shown in figure 6 (b). For this reason, the amplitude of the distortion is small but the sample is completely distorted.

The formalism we have developed can be used to analyse many situations in closed analytical form. Here, we have focused only on some particular examples to illustrate the usefulness of the approach in facing real situations. A link between these calculations and experimental results can be made by considering the optical path difference, which allows one to investigate the orientational states of the system. When $\theta(x, z)$ is known, as in the formalism we have proposed above, the physical properties of a NLC sample can be explored. For instance, the optical path difference Δl, between the ordinary and extraordinary ray [1], is given by

$$\Delta l = \frac{1}{\Lambda}\int_{-\Lambda/2d}^{\Lambda/2d}\int_{-1/2}^{1/2} \Delta n(\theta)\mathrm{d}x\,\mathrm{d}z = \frac{1}{2} n_0 R\, d\langle\theta^2\rangle, \qquad (34)$$

where

$$\langle\theta^2\rangle = \frac{d}{\Lambda}\int_{-\Lambda/2d}^{\Lambda/2d}\int_{-1/2}^{1/2} \theta^2(x, z;\ t)\mathrm{d}x\,\mathrm{d}z, \qquad (35)$$

is the average square tilt angle, evaluated over a typical length Λ, connected with the diameter of the light beam. Moreover, $R = 1-(n_0/n_e)^2$, where n_0 and n_c are the ordinary and extraordinary refractive indices, respectively. This completes the formalism to determine, in an exact manner, the tilt angle profile and the dynamics of its orientation under the action of an external field in a situation in which only splay–bend distortion is allowed for the system.

5. Summary and conclusion

The dynamics of the director reorientation have been investigated for a NLC sample of thickness d, under the action of an external time-dependent field, when only splay–bend deformation is allowed in the system. The general results, given in terms of Green's function, have been applied to some illustrative examples. In one of these examples, one surface is characterized by a periodic distribution of easy axes. The particular importance of the present approach is to consider a space–time-dependent distribution of the easy axes, because, in this general situation, the spatial inhomogeneities of the surface as well as the evolution with time of the easy direction can be taken into account in a unified way. This general situation can be relevant for those systems in which the surfaces are covered by photopolymeric films whose orientation is fully determined by the previous treatment of the polymer. Therefore, by illumination, the configuration at the surface can be controlled externally while the dynamics of the director can be exactly determined for small distortions near the threshold field, when an external time-dependent electric field is applied on the system.

Acknowledgements

This work was partially supported by Brazilian Agencies Capes, CNPq (Instituto do Milênio de Fluidos Complexos) and Fundação Araucária.

References

[1] G. Barbero, L.R. Evangelista. *An Elementary Course on the Continuum Theory for Nematic Liquid Crystals*, World Scientific, Singapore (2001).
[2] I.W. Stewart. *The Static and Dynamical Continuum Theory of Liquid Crystals*, Taylor & Francis, London (2004).
[3] J.L. Ericksen. *Adv. Liq. Cryst.*, **2**, 233 (1976).
[4] J.L. Ericksen. *Arch. Ration. Mech. Anal.*, **4**, 231 (1960).
[5] J.L. Ericksen. *Trans. Soc. Rheol.*, **5**, 23 (1961).
[6] J.L. Ericksen. *Arch. Ration. Mech. Anal.*, **9**, 371 (1962).
[7] F.M. Leslie. *Adv. Liq. Cryst.*, **4**, 1 (1979).
[8] F.C. Frank. *Discuss. Faraday Soc.*, **25**, 19 (1958).
[9] C.W. Oseen. *Trans. Faraday Soc.*, **29**, 883 (1933).
[10] G. Lester, S. Coulston. *Mol. Cryst. Liq. Cryst.*, **433**, 117 (2005).
[11] C.L. Chen. *Tamkang J. Sci. Eng.*, **7**, 5 (2004).
[12] H.L. Ong, *et al. J. Appl. Phys.*, **57**, 186 (1984).
[13] L. Janossy, T.I. Kosa. *Phys. Rev. E*, **70**, 052701 (2004).
[14] G. Barbero. *Lett. Nuovo Cimento*, **29**, 553 (1980).
[15] G. Barbero. *Lett. Nuovo Cimento*, **32**, 60 (1981).
[16] G. Barbero, T. Beica, A.L. Alexe-Ionescu, R. Moldovan. *J. Phys. (Paris) II*, **2**, 2011 (1992).
[17] L.R. Evangelista, G. Barbero. *Phys. Rev. E*, **48**, 1163 (1993).
[18] L.R. Evangelista, G. Barbero. *Phys. Rev. E*, **50**, 2120 (1994).
[19] C.A.R. Yednak, F.C.M. Freire, E.K. Lenzi, L.R. Evangelista. *Liq. Cryst.*, **33**, 409 (2006).
[20] C.A.R. Yednak, F.C.M. Freire, E.K. Lenzi, L.R. Evangelista. *Phys. Rev. E*, **72**, 042701 (2005).
[21] A. Rapini, M.J. Papoular. *J. Phys. Coll.*, **30**, 54 (1969).
[22] V. Fréedericksz, V. Zolina. *Trans. Faraday Soc.*, **29**, 919 (1933).
[23] P. Pagliusi, G. Cipparrone. *Phys. Rev. E*, **69**, 061708 (2004).
[24] G. Barbero, L.R. Evangelista. *Adsorption Phenomena and Anchoring Energy in Nematic Liquid Crystals*, Taylor & Francis, London (2006).
[25] P.G. de Gennes. *The Physics of Liquid Crystals*, Clarendon Press, Oxford (1974).
[26] G. Vertogen, W.H. de Jeu. *Thermotropic Liquid Crystals, Fundamentals*, Springer, Berlin (1988).

[27] S. Chandrasekhar. *Liquid Crystals*, Cambridge Univeristy Press, Cambridge (1977).
[28] M. Kléman. *Points, Lignes, Parois* Editions de Physique, Les Ulis, Orsay (1977).
[29] E. Butkov. *Mathematical Physics*, Addison-Wesley, New York (1968).
[30] P.M. Morse, H. Feshbach. *Methods of Theoretical Physics,* Vol. I, Ch. 8, McGraw-Hill, New York (1953).